Blast wave attenuation by lightly destructable granular materials

V.V. Golub[1], F.K. Lu[2], S.A. Medin[1], O.A. Mirova[1], A.N. Parshikov[1], V.A. Petukhov[1], and V.V. Volodin[1]

[1] *Institute for High Energy Densities, Associated Institute for High Temperatures, Izhorskaya 13/19, Moscow 125412, Russia.*
[2] *Aerodynamics Research Center, University of Texas in Arlington, Arlington, TX, USA.*

1 Introduction

Terrorist bombings are a dismal reality nowadays. One of the most effective ways for protection against blast overpressure is the use of lightly compacted materials such as sand [1] and aqueous foam [2] as a protective envelope or barrier. According to [1], shock wave attenuation in a mine tunnel (one-dimensional case) behind a destroyed object is given by

$$q_e \approx q \frac{1}{1 + 4(S/q)^{1/6} b \rho_{mat} / L^{1/3}} \tag{1}$$

where q_e - effective charge, S - exposed area of the obstacle, q - TNT equivalent (grams), L - distance between charge and obstacle, b - obstacle thickness and ρ_{mat} - material density. This empirical equation is applicable only in a one-dimensional case but not for a less confined environment. Another way of protecting a structure against blast is to coat the surface with a sacrificial layer. In [3] full-scale experiments were carried out to investigate the behaviour of a covering of aluminum foam under the effect of a blast wave. In our study, a sand/cement mixture is proposed as a material for structural protection by absorbing the energy of the explosion, thereby helping to attenuate the blast. Moreover, this material does not produce shrapnel since it is pulverized under the action of the blast wave.

2 Experiment

The explosions were produced in a cylindrical steel chamber $VBK - 2, 4.5m$ in diameter and $7m$ in length. The sand/cement cylinder was placed $95cm$ above the ground on the axis of a chamber. The wall thicknesses of the cylinders were $13, 9$ and $5cm$. The cylinder were madeof a $15 : 1$ sand/cement mixture. Explosive charge was placed in the center of a cylinder. Pressure transducers were installed in the chamber to determine the total and static pressures. The total and static pressure transducers were installed at fixed distances L from the center of the charge. Fig. 2.1 shows the disposition of the gauges in the third experiment. Explosives used were 200 g of hexogen (equivalent of 266 g TNT) in the first experiment while 200 g of ammonite (equivalent to 226 g of TNT were used in the second and third experiments.

2.1 Experimental Results

Tables 1–3 (cylinder wall thickness of 9, 13 and 5 cm respectively) show data obtained in the experiments. In the tables L is the distance between the epicenter and pressure

transducer, τ is the time interval from initiating the explosion to the moment of blast wave arrival at the transducer in the case of a 'confined' blast (i.e., with the presence of the sand/cement cylinder), ΔP_{oa} is the pressure recorded by the transducer in case of an open-air explosion and ΔP_c is the pressure in the case of a 'confined' explosion. The blast wave attenuation coefficient is $K = \Delta P_{oa}/\Delta P_c$. In Fig. 2, the trajectory of the blast wave in the case of an open-air explosion (triangles), the trajectory of the blast wave for an explosion with the sand/cement attenuator (diamonds) and the trajectory of the sand front are presented. As was expected, the velocity of the blast wave in the first case was higher than that with the attenuator. Figure 3 presents the decrease of the blast wave attenuation coefficient with effective distance and the dependence of the attenuation coefficient on wall thickness. As may be seen, an increase of cylinder wall thickness from 8 to 13 cm does not increase the attenuation coefficient.

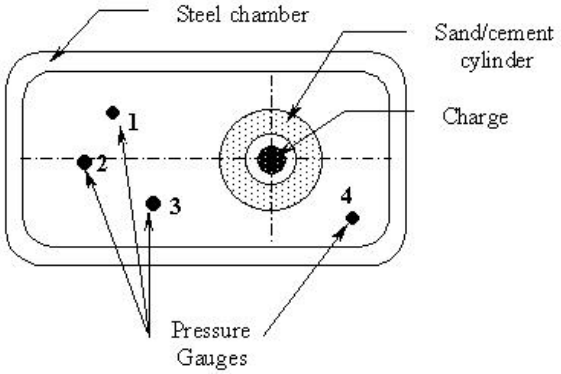

Fig. 1. Schematic of disposition of charge and transducers in the experiment

Table 1. Experiment 1: 1, 2, 4 - total pressure; 3, 5 - static pressure

	L, m	τ, ms	$\Delta P_{oa}, bar$	ΔP_c, bar	K
1	3.53	8.64	0.167	0.078	2.13
2	2.76	6.32	0.3	0.14	2.13
3	1.98	4.28	1.87	0.52	3.57
4	1.63	2.64	2.81	1.06	2.63
5	3.48	7.2	0.71	0.37	1.92

3 Numerical simulation and comparison with experiment

3.1 Computational method and testing with open air blast

Propagation of shock waves in open air and pressure profiles at gauge locations were computed by the code SPH [4]. In this code, 2D axisymmetrical hydrodynamic equations

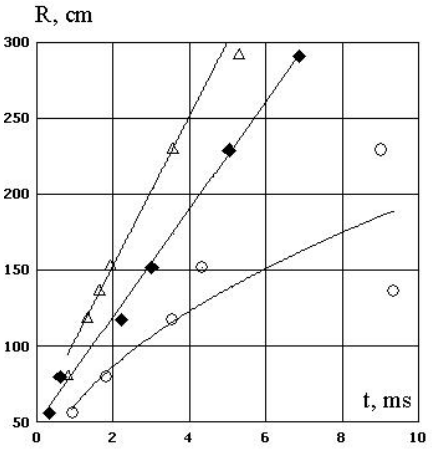

Fig. 2. The trajectory of blast wave for explosion without attenuator (triangles), the trajectory of blast wave for explosion with sand attenuator (diamonds) and trajectory of the sand front

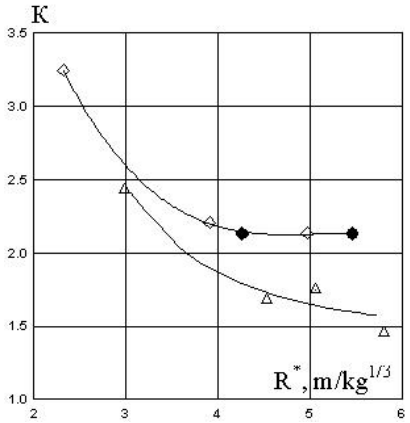

Fig. 3. The attenuation parameters: R^* - distance to epicenter normalized by equivalent TNT charge, K - attenuation coefficient (diamonds - 13 cm wall, circles - 8 cm wall, triangles - 5 cm wall)

Table 2. Experiment 2: 1-3 - static pressure

	L, m	τ, ms	ΔP_{oa}, bar	ΔP_c, bar	K
1	2.29	5.03	0.269	0.122	2.22
2	2.91	6.87	0.305	0.143	2.13
3	1.36	6.87	0.837	0.257	3.23

Table 3. Experiment 3: 1-4 - static pressure

	L, m	τ, ms	ΔP_{oa}, bar	ΔP_c, bar	K
1	2.96	6.76	0.198	0.113	1.75
2	3.39	8.26	0.30	0.021	1.45
3	2.65	6.02	0.18	0.107	1.69
4	1.74	3.78	0.65	0.27	2.43

are solved by means of Lagrangian smoothed particles, being adapted to local peculiarities of the flow field. The code algorithm was improved by means of adaptive splitting and sticking of SPH particles.

In the computations, the detonation period was passed over by substitution of condensed explosive in the initial cells by detonation products at a certain pressure

$$P_H = \frac{\rho_H D^2}{2(\gamma+1)}, \tag{2}$$

where $\gamma = 3$, $\rho_H = 1.2$ cm^3, $D = 6500$ m/s. Therefore, an instantaneous detonation was assumed. The equation of state for the detonation products was taken as for a perfect gas

$$P = (\gamma - 1)\rho e \tag{3}$$

The pressures measured by the gauges were related to the pressures computed in the cells nearest to the gauge. Smoothing of the pressure values taken from the surrounding array of cells was not required because of the good monotonicity of the numerical solution. The gauge bodies were not presented in the computational region and, therefore, their influence on the flow field was neglected.

The code was tested with experimental data for explosion of 200 g of hexogen in air. Comparison with computations is presented in Fig. 4. Gauges $D3$–$D5$ measured the total pressure, which exceed the pressure at the shock front. The computed shock is relatively weak for the rule of doubling of pressure rise at the normal reflection to be applied. In Fig. 4, the doubled values of pressure rise at the gauges $D3$–$D5$ are plotted. The comparison of the measured and computed data validites the code.

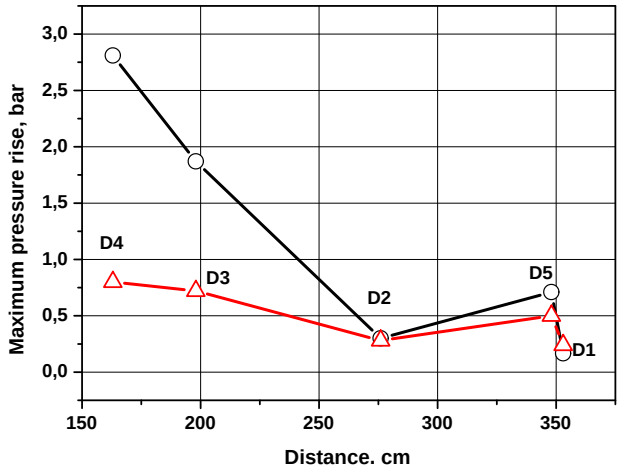

Fig. 4. Maximum pressure rise for TNT explosion in open air at static pressure gauges $D1$, $D2$ and total pressure gauges $D3$–$D5$. Measured values (◯), computed values (△).

3.2 Simulation of explosion in sand/cement cylinder

An important point in the simulation of explosion in sand/cement cylinder is choice of an equation of state heterogeneous medium, i.e. sand/air, and the strength properties of the initial phase of cylinder failure. In this simulation we take into account only the first factor. Following [4] we use an equation of state that combines properties of liquid and gas

$$P = C_B^2(\rho - \rho_0)\delta + (\gamma - 1)\rho e, \tag{4}$$

where $C_B = 1280$ m/s, $\rho_0 = 2200$ kg/m^3, $\gamma = 3$, $\delta = 1 \bigvee 0$ for $\rho \leq \rho_0$ or $\rho > \rho_0$, respectively. The maximum pressure rise at the gauges is presented in Fig. 6. Figure 5

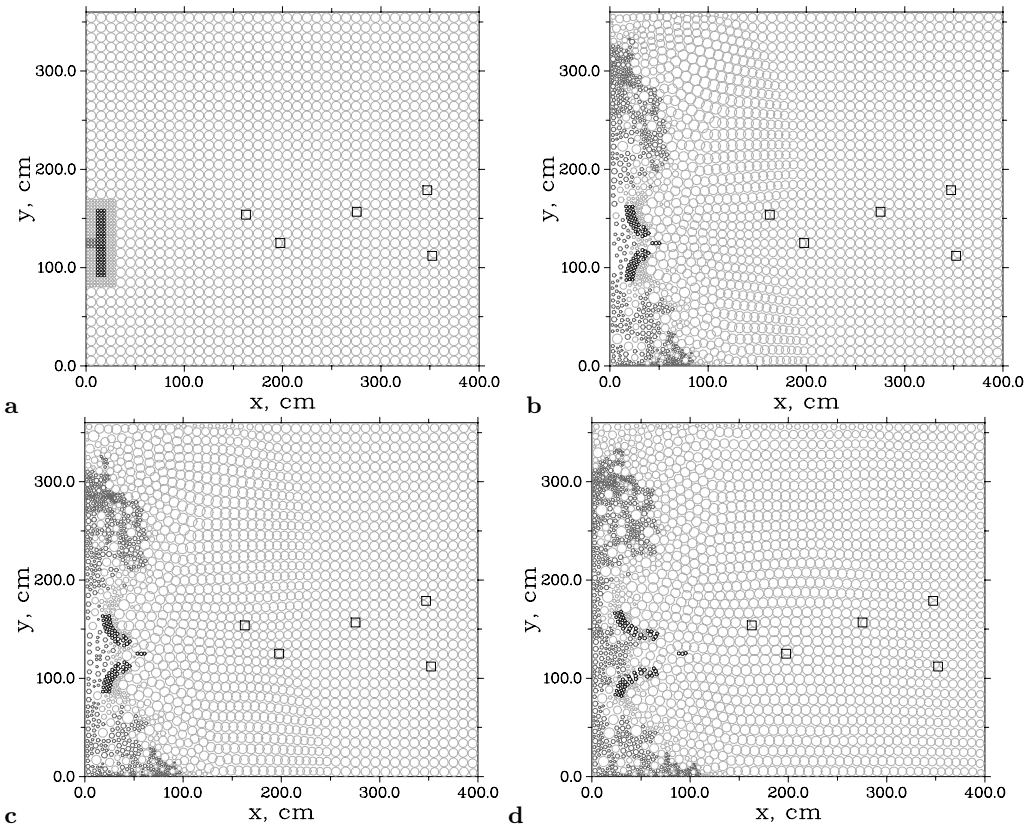

Fig. 5. Flow fields for 'confined' TNT explosion. Time moments 0.0, 2.6, 3.5 and 6.5 ms correspondingly. The pressure transducers positions are marked by squares. The material is presented by black circles for the sand/cement cylinder, by dark-grey circles for detonation products and light-grey circles for air. Left border is symmetry axis, other borders are chamber walls.

shows that the temporal responses of the gauges in the numerical simulation and the experiment are quite similar except for gauge $D4$. The gauges are affected mainly by reflected shocks and this leads to the noticeable time reduction and pressure amplitude increase at the gauges positions in computations.

We can assume that in the experiment the detonation shock penetrated partially through the destroyed sand cylinder and was recorded by the gauges.

For the gauges $D4$ and $D3$, a substantial decrease of the computed data compared to the measured values is observed. The authors attribute this discrepancy to rather rough discretization of computational area relative to the width of the pressure pulse. The pressure pulse is spread because of the numerical viscosity of the scheme. For a short enough pulse, this spreading leads to decrease of the pressure amplitude, while impulse in conserved. This takes place for the near gauges $D4$ and $D3$. For the remote gauges, the width of the pulse is larger and agreement between measured and computed data are good.

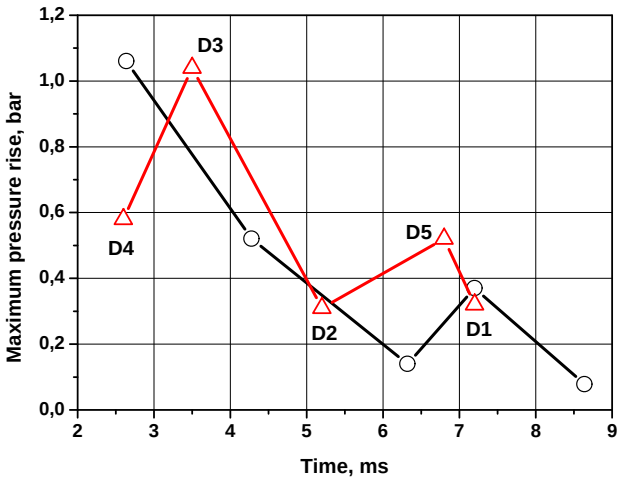

Fig. 6. Maximum pressure rise for TNT explosion in sand/cement cylinder at static pressure gauges $D1$, $D2$ and total pressure gauges $D3$–$D5$. Measured values (◯) and computed values (△).

4 Conclusions

- A special filler was proposed for fail-safe construction techniques for protecting the buildings from terrorist-type explosions.
- Experimental results showed that a wall made of weak sand/cement composition (1:15 by weight) is pulverized by the explosion and the sand scatters within a distance of 3 m.
- Measured coefficient of attenuation of blast wave was 1.75–3.23.

Acknowledgement. Research partly funded by the U.S. Civilian Research and Development Foundation, Grant No. RE2-2481-MO-02.

References

1. G.I. Pokrovsky: *Explosion.* (Nedra, Moscow 1980)
2. A.A. Borisov, B.E. Gelfand, V.M. Kudinov, B.I. Palamarchuk, V.V. Stepanov, E.I. Timofeev, S.V. Khomik: Shock waves in water foams. Acta Astron. **5(11-12)**, 1027 (1978)
3. A.G. Hanssen, L. Enstok, M. Langseth: Close-range blast loading of aluminum foam panels. Int J Impact Engg **27(11-12)**, 593 (2002)
4. H.J. Melosh: *Impact Cratering. A Geologic Process.* (Oxford, New York, 1989)
5. A.N. Parshikov: Application of a solution to the Riemann problem in the SPH method. Comput Math Mathem Phys **39(7)**, 1216 (1999)
6. A.N. Parshikov, S.A. Medin, I.I. Loukashenko, V.A.Milekhin: Improvements in SPH method by means of interparticle contact algorithm and analysis of perforation tests an moderate projectile velocities. Int J Impact Engg **24**, 779 (2000)
7. A.N. Parshikov, S.A.Medin: Smoothed particle hydrodynamics using interparticle contact algorithms. J Comput Phys **180**, 358 (2002)